

Combinatorial-hybrid Optimization for Multi-agent Systems under Collaborative Tasks

Zili Tang, Junfeng Chen and Meng Guo

Abstract—Multi-agent systems can be extremely efficient when working concurrently and collaboratively, e.g., for transportation, maintenance, search and rescue. Coordination of such teams often involves two aspects: (i) selecting appropriate sub-teams for different tasks; (ii) designing collaborative control strategies to execute these tasks. The former aspect can be combinatorial w.r.t. the team size, while the latter requires optimization over joint state-spaces under geometric and dynamic constraints. Existing work often tackles one aspect by assuming the other is given, while ignoring their close dependency. This work formulates such problems as combinatorial-hybrid optimizations (CHO), where both the discrete modes of collaboration and the continuous control parameters are optimized simultaneously and iteratively. The proposed framework consists of two interleaved layers: the dynamic formation of task coalitions and the hybrid optimization of collaborative behaviors. Overall feasibility and costs of different coalitions performing various tasks are approximated at different granularities to improve the computational efficiency. At last, a Nash-stable strategy for both task assignment and execution is derived with provable guarantee on the feasibility and quality. Two non-trivial applications of collaborative transportation and dynamic capture are studied against several baselines.

I. INTRODUCTION

Fleets of heterogeneous and autonomous robots are deployed nowadays to accomplish tasks that are otherwise too inefficient or even infeasible for a single robot, e.g., collaborative transportation [1], [2], dynamic capture [3] and surveillance [4]. Both the overall efficiency and capability of the team are significantly improved by allowing the team of robots to act concurrently and collaboratively. Two aspects are often involved for the coordination of such teams. On the one hand, the given set of tasks could be accomplished by various subgroups of the team, however at drastically different costs [5], [6], [7]. For instance, three agents can detect and capture a dynamic target much faster than one agent (if possible at all), while five agents might be redundant in certain scenarios. Thus, an appropriate task assignment is crucial for the overall performance, which unfortunately often has a complexity combinatorial to the number of agents and tasks. On the other hand, given certain assignments, how each subgroup executes the assigned task often boils down to an optimal control problem [2], [8], i.e., how to actuate the agents collaboratively to minimize the cost associated with a task, under the dynamic and geometric constraints [6],

[9]. Exact optimization has a high complexity due to the long horizon and the high dimension of joint-state-control space of all collaborators. Lastly, there is often a “chicken or the egg” dilemma w.r.t. these two aspects [10], [11]. Namely, the task assignment relies on the optimal control to evaluate feasibility and actual cost, while the optimal control problem requires certain assignments as inputs. Solving first the control problems for *all* possible assignments and then the task assignment problem is mostly intractable, as it multiplies the complexity of both aspects.

A. Related Work

Task planning for multi-agent systems refers to the process of first decomposing this task into sub-tasks and then assigning them to the team, see [5], [6], [12] for comprehensive surveys. Different optimization criteria can be chosen, typically: MinSUM that minimizes the sum of agent costs over all agents [6], [13]; and MinMAX that minimizes the maximum cost of all agents [14]. Well-known problems include the classic one-to-one assignment problem [15], the multi-Vehicle routing problem [6], [12], and the coalition formation problem [7], [16]. Representative methods include the Hungarian method [15], the mixed integer linear programming (MILP) [5], the search-based methods [13]; and the market-based methods [12]. However, this body of literature normally assumes a static and known table of task-per-agent costs, which is not always available or even *invalid* for collaborative tasks, as the benefit of one agent joins a task depends on which other agents also participate.

Motion planning for multi-agent systems refers to the design of control strategies for each agent to accomplish a given task. One common task is the collaborative navigation where each agent navigates to its goal position while avoiding collision with other agents or obstacles, see [17], [9]. Other tasks such as formation, flocking are also studied under various constraints, see [18]. Another relevant task is the collaborative load transportation [19], [20], where several agents transport one object to the destination via pushing or grasping. These motion planning problems remain challenging due to the dynamic and geometric constraints associated with different tasks. Moreover, these works mostly assume a global objective for the whole team, i.e., without the need for decomposing and assigning subtasks.

Integrating the above two aspects yields a task and motion planning (TAMP) problem for multi-agent systems [21], [22]. The work in [11] proposes a combination of receding horizon-based task decomposition and motion planning for autonomous assembly. Similarly, a furniture-assembly

The authors are with the College of Engineering, Peking University, Beijing 100871, China. This work was supported by the National Natural Science Foundation of China (NSFC) under grants 62203017, T2121002, U2241214; and by the Fundamental Research Funds for the central universities. Contact: tang.zili, chenjunfeng, meng.guo@pku.edu.cn.

task is considered in [23] where re-grasps are introduced to decompose the long-horizon assembly operations. Both works put strong emphases on the physical stability and sequential feasibility during collaborative manipulation, while neglecting the combinatorial aspect as only a few agents are considered. The classic game of “cops and robbers” is considered in [3], [24] where multiple pursuers are tasked to capture multiple evader. The proposed solutions decouple the task assignment and the controller design by adopting a greedy assignment policy, e.g., nearest target [3] or maximum matching pairs [24]. Thus, there remains a need for an integrated solution for multi-agent TAMP problems that can tackle simultaneously the combinatorial task assignment and the collaborative control design.

B. Our Method

To overcome these challenges, this work proposes a combinatorial-hybrid optimization (CHO) framework for multi-agent systems under collaborative tasks. Several agents can collaborate on one common task as a coalition, the cost of which depends not only on the number of participants, but also the mode of collaboration and the underlying control parameters. Thus, the proposed framework includes two layers: (i) the optimization of coalition structure, and (ii) the hybrid search of optimal collaborative behavior as the sequence of discrete modes and continuous control parameters. Both layers are performed concurrently and in-demand, i.e., the hybrid search for a given task coalition is solved for the actual cost, only when such a coalition is demanded promising during task assignment. It is shown that the final solution of coalition structure and the associated collaborative behavior is Nash-stable. To demonstrate its applicability, two non-trivial multi-agent collaborative tasks, including collaborative transportation and dynamic capture, are modeled and solved via the proposed framework.

Main contribution of this work lies in two aspects: (i) the formulation of combinatorial-hybrid optimization problems for multi-agent systems under collaborative tasks, particularly for scenarios where the agent-per-task costs do not exist and can only be derived after solving a hybrid optimization problem; (ii) the proposed framework finds simultaneously the coalition formation and the optimal collaborative behaviors, with a provable quality guarantee.

II. PROBLEM DESCRIPTION

A. Model of Workspace and Agents

Consider a team of N agents that collaborate in a shared workspace, denoted by $\mathcal{X} \subset \mathbb{R}^X$. The system state $x \in \mathcal{X}$ includes not only the agent states but also other dynamic components such as movable objects and targets. Due to the dynamic and geometric constraints such as collision avoidance among the agents and with obstacles, the system is required to stay within the allowed subset $\mathcal{X}_{\text{safe}} \subset \mathcal{X}$.

B. Parameterized Modes

Moreover, these agents can change the system state by numerous *parameterized modes*, denoted by $\Xi \triangleq \{\xi_1, \dots, \xi_K\}$.

Under each mode $\xi_k \in \Xi$, the system state evolves under a closed-loop dynamics $h_k : \mathcal{X} \times 2^{\mathcal{N}} \times \mathbb{R}^{P_k} \rightarrow \mathcal{X}$, i.e.,

$$x(t+1) \triangleq h_k(x(t), \mathcal{N}_k, \rho_k), \quad \forall t \in [t_0, t_0 + T_k], \quad (1)$$

where $k \in \mathcal{K} \triangleq \{1, \dots, K\}$ for one valid mode; $\mathcal{N}_k \subseteq \mathcal{N}$ is a subset of agents that participate in this mode (called coalitions); $\rho_k \in \mathbb{R}^{P_k}$ is the continuous parameter chosen for this mode with dimension P_k ; $x(t)$ and $x(t+1)$ are the system states before and after agents in \mathcal{N}_k perform mode ξ_k with parameter ρ_k for one time step; $t_0 \geq 0$ is an arbitrary starting time; T_k is a given minimum duration of mode ξ_k . For performance measure, there is a cost function $c_k : \mathcal{X} \times 2^{\mathcal{N}} \times \mathbb{R}^{P_k} \rightarrow \mathbb{R}^+$ associated with each mode ξ_k under a particular choice of (\mathcal{N}_k, ρ_k) . It is assumed in this work that the functions h_k, c_k above associated with each mode $\xi_k \in \Xi$ is accessible either via explicit functions or numerical simulations. Such modes are often built upon well-established functional modules that are designed beforehand for specific and simpler purposes. More examples for two different applications can be found in Sec. III.

C. Collaborative Tasks

Furthermore, there are M tasks specified for the team, denoted by $\Omega \triangleq \{\omega_1, \dots, \omega_M\}$. Each task $\omega_m \in \Omega$ in the most general sense is to change the system state to a set of goal states $\mathcal{X}_{G_m} \in \mathcal{X}$. Each task can be accomplished by a *hybrid plan* as a sequence of modes with appropriate choices of coalitions and parameters, i.e.,

$$\varphi_m \triangleq (\xi_{k_1^m}, \mathcal{N}_{k_1^m}, \rho_{k_1^m}) \cdots (\xi_{k_L^m}, \mathcal{N}_{k_L^m}, \rho_{k_L^m}), \quad (2)$$

where $L > 0$ is the total number of modes to be optimized; and $(\mathcal{N}_{k_\ell^m}, \rho_{k_\ell^m})$ are permissible coalitions and parameters according to function h_{ξ_k} in (1) for each mode $\xi_{k_\ell^m} \in \Xi$, $\forall \ell = 1, \dots, L$. Thus, the evolution of system state under plan φ_m is constrained by:

$$\begin{aligned} x_{k_\ell^m} &= h_{k_\ell^m}(x_{k_{\ell-1}^m}, \mathcal{N}_{k_\ell^m}, \rho_{k_\ell^m}); \\ x_{k_0^m} &= x_0, \quad x_{k_L^m} \in \mathcal{X}_{G_m}, \end{aligned} \quad (3)$$

where $x_0 \in \mathcal{X}$ is a given initial state. The associated cost of φ_m is given by the accumulated cost, i.e., $c(\varphi_m) \triangleq \sum_{\ell} c_{k_\ell^m}(x_{k_{\ell-1}^m}, \mathcal{N}_{k_\ell^m}, \rho_{k_\ell^m})$, which holds for each $\omega_m \in \Omega$. In addition, since different modes can be executed in a concurrent way for different tasks, it is assumed in this work that different tasks change different dimensions of the state in an independent way, i.e.,

$$x(t+1) = x(t) + \sum_{\omega_m \in \Omega} \left(h_{k_t^m}(x(t), \mathcal{N}_{k_t^m}, \rho_{k_t^m}) - x(t) \right), \quad (4)$$

where $\xi_{k_t^m} \in \Xi$ is the active mode of task ω_m at time $t \geq 0$; $(\mathcal{N}_{k_t^m}, \rho_{k_t^m})$ is the associated coalition and parameter; $x(t)$ is the current system state; and $x(t+1)$ is the resulting state after executing all active modes for one time step. Lastly, since each agent can only participate in maximal one task for all time, it holds that:

$$\mathcal{N}_{m_1}(t) \cap \mathcal{N}_{m_2}(t) = \emptyset, \quad \forall \omega_{m_1}, \omega_{m_2} \in \Omega; \quad (5)$$

where $\mathcal{N}_{m_1}(t), \mathcal{N}_{m_2}(t)$ denote the coalitions responsible for executing any two tasks $\omega_{m_1}, \omega_{m_2} \in \Omega$ at time $t \geq 0$.

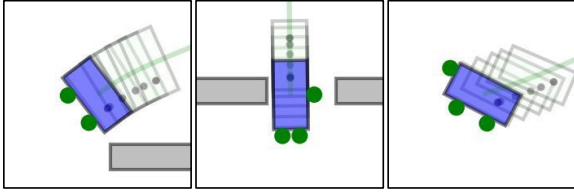


Fig. 1. Illustration of three different modes for the use case of object transportation described in Sec. III-A: Long-Side Pushing (**Left**), Short-Side Pushing (**Middle**), and Diagonal Pushing (**Right**).

D. Combinatorial-hybrid Optimization (CHO)

Problem 1. Given the above model of N agents and M tasks, the complete combinatorial-hybrid optimization (CHO) problem is defined as follows:

$$\begin{aligned} \min_{\{\varphi_m\}} \quad & \left\{ \max_m \{c(\varphi_m)\} + \frac{1}{M} \sum_m c(\varphi_m) \right\} \quad (6) \\ \text{s.t.} \quad & (3) - (5), \forall \ell, \forall m; \end{aligned}$$

where $\{\varphi_m\}$ is the set of hybrid plans for all tasks; the objective is to minimize a balanced cost between the maximum cost and the average cost among all tasks; (3)-(5) are the dynamic and geometric constraints associated with the system state and the structure of coalitions. ■

III. TWO CONCRETE USE CASES

To clarify the problem formulation described in Sec. II, two use cases of multi-agent systems that can be modeled by the CHO framework are presented first in this section, of which the detail setup and results are given in Sec. V.

A. Collaborative Transportation

Consider the problem in which a team of N agents is tasked to move M identical rectangular boxes from their initial positions to target positions in a cluttered workspace, as illustrated in Fig. 1. The state of a box is determined by its center (x_m, y_m) and its orientation ψ_m , of which the target position is given by (x_m^*, y_m^*) .

The agents can make contact at specific points on the box and push it forward by applying pushing forces $F_n \in [0, F_{\max}]$. Different combinations of contact points result in different system dynamics thus different modes $\Xi = \{\xi_k\}$. As shown in Fig. 1, the box can be pushed by different number of agents in different modes, where the parameters are the applied forces $\rho_k = \{F_n\}$. Clearly, more agents lead to a higher degree of controllability and faster motion. Moreover, a sequence of different modes with distinct parameters might be required to move a box to its target position, e.g., through narrow passages and sharp corners.

B. Dynamic Capture

Consider the problem of dynamic capture that involves N pursuers and M evaders in a cluttered 2D workspace. Their states and velocities are denoted by $(x_n(t), v_n(t))$ and $(y_m(t), v_m(t))$. The agents all have the *same* maximum velocity v_{\max} , meaning that collaborations are required for the pursuers to catch the evaders. There is a capture task

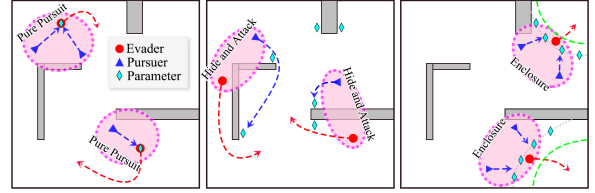


Fig. 2. Illustration of three different modes associated with the use case of dynamic capture described in Sec. III-B: Pure Pursuit (**Left**), Hide and Attack (**Middle**), and Enclosure (**Right**).

associated with each evader, which moves in the opposite direction of all pursuers, weighted their relative distances.

In addition, as shown in Fig. 2, there are three parameterized modes $\Xi = \{\xi_1, \xi_2, \xi_3\}$ for each task: (i) *Pure Pursuit*. The pursuers follow the “line-of-sight” strategy to move towards the assigned evader, i.e., $v_n = v_{\max} \text{point}(\{x_n\}, \rho_1)$ as the unit vector from x_n to the parameter $\rho_1 \in \mathbb{R}^2$ determined by the position of assigned evader. (ii) *Hide and Attack*. The pursuers conceal themselves behind obstacles until the assigned evader appears, and then encircle it, i.e., $v_n = \text{nav}(\{x_n\}, \rho_2)$ as a navigation function that guides the pursuer to a hiding or attacking position $\rho_2 \in \mathbb{R}^2$. (iii) *Enclosure*. The pursuers drive the assigned evader into a corner by reducing the region of advantage [25] for the evader until it is captured, i.e., $v_n = \text{corner}(\{x_n\}, \rho_3)$ as an optimization algorithm that generates the optimal velocity given other pursuers $\{x_n\}$ and key position $\rho_3 \in \mathbb{R}^2$. Consequently, each pursuer should choose a sequence of modes, coalitions and the associated parameters, to capture all evaders as fast as possible.

IV. PROPOSED SOLUTION

The proposed solution tackles Problem 1 via two interleaved and concurrent layers: (i) coalition formation, and (ii) hybrid optimization of collaborative behaviors. The first layer proposes candidates of coalitions for each task to minimize the overall cost. These candidates are then sent to the second layer which solves a constrained hybrid optimization for each coalition, to determine the optimal hybrid plans and actual cost to accomplish the assigned task. These costs are then fed back to the first layer to adjust existing coalitions. This process repeats itself until a Nash-stable solution is found. Each layer is described in detail in this section.

A. Coalition Formation

1) *Problem of Coalition Formation*: The first layer assigns the set of tasks to available agents. To begin with, the task assignment problem is formulated based on the literature of coalition formation [26], [27]. Particularly, consider the coalition structure defined as follows:

$$\mathcal{F} \triangleq (\mathcal{R}, \Omega, f), \quad (7)$$

where $\mathcal{R} = \{1, \dots, N\}$ is the team of N agents; $\Omega = \{\omega_1, \dots, \omega_M\}$ is the set of M tasks; $f : 2^{\mathcal{R}} \times \Omega \rightarrow \mathbb{R}^+$ is the cost function of a potential coalition for any given task in Ω . Note that since the exact cost f above is often

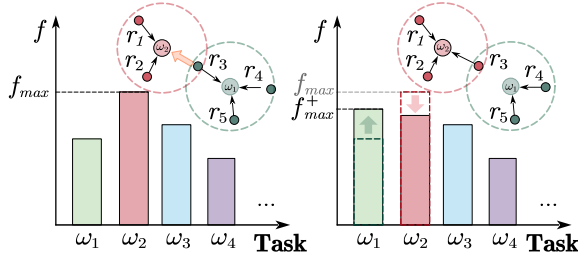


Fig. 3. Illustration of the coalition formation algorithm in Sec. IV-A.2. Agents switch coalitions to reduce the overall cost in (8).

unknown, thus estimated initially by simple heuristics such as Euclidean distance, denoted by f .

Definition 1 (Assignment). A valid solution of the coalition structure \mathcal{F} in (7) is called an assignment, denoted by $\mu = \{(\mathcal{R}_m, \omega_m), \forall \omega_m \in \Omega\}$, where $\mathcal{R}_m \subset \mathcal{R}$ is a coalition that performs the common task $\omega_m \in \Omega$, and $\mathcal{R}_{m_1} \cap \mathcal{R}_{m_2} = \emptyset, \forall m_1 \neq m_2$. Moreover, the estimated cost is given by:

$$C(\mu) \triangleq \max_{\omega_m \in \Omega} \{\hat{f}_m\} + \frac{1}{M} \sum_{\omega_m \in \Omega} \hat{f}_m, \quad (8)$$

where $\hat{f}_m \triangleq \hat{f}(\mathcal{R}_m, \omega_m)$ is the estimated cost of each coalition; and $C(\cdot)$ is a balanced cost based on (6). ■

Let $\mu(\omega_m) = \mathcal{R}_m$ return the coalition for task ω_m and $\mu(n) = \omega_m$ return the task assigned to agent $n, \forall n \in \mathcal{R}_m$. More importantly, an assignment μ can be modified via the following switch operation.

Definition 2 (Switch Operation). The operation that agent $n \in \mathcal{R}$ is assigned to task $\omega_m \in \Omega$ is called a switch operation, denoted by σ_n^m . The switch σ_n^m is valid only if agent n can perform task ω_m . Thus, an assignment μ is changed into a new assignment $\hat{\mu}$ via σ_n^m such that $\hat{\mu}(n) = \omega_m$. For brevity, denote by $\hat{\mu} = \sigma_n^m(\mu)$. ■

Definition 3 (Nash Stable). An assignment μ^* is called Nash-stable, if there does not exist any switch operation σ_n^m such that $C(\sigma_n^m(\mu^*)) < C(\mu^*)$ by (8), $\forall n \in \mathcal{N}$. ■

Given the above definitions, the first layer of coalition formation is transformed into the problem of finding a Nash-stable assignment as follows.

Problem 2. Given a coalition structure \mathcal{F} in (7), find one Nash-stable assignment μ^* by Def. 3. ■

2) *Dynamic Task Assignment:* The proposed solution follows an iterative switching operations to reduce the largest cost of all tasks. An initial assignment μ_0 can be derived in a random or greedy way. Then, the *target* coalition with the k -th maximum cost is selected via:

$$(\mathcal{R}_{m^*}, \omega_{m^*}) = \operatorname{argmax}_{(\mathcal{R}_m, \omega_m) \in \mu_0}^{[k]} \{\hat{f}_m\}, \quad (9)$$

where $k = 1$ initially for the maximum cost; and ties are broken arbitrarily. Given $(\mathcal{R}_{m^*}, \omega_{m^*})$, the first step is to calculate the *actual* utility f_{m^*} , via the hybrid optimization procedure described in the subsequent section. There are two possible outcomes: (I) If $f_{m^*} \geq \max_{m \neq m^*} \{\hat{f}_m\}$, it

means that ω_{m^*} remains the target coalition. As illustrated in Fig. 3, the goal is to find a switch operation $\sigma_n^{m^*}$ for one agent $n \in \mathcal{N}$ such that after applying $\sigma_n^{m^*}$ the maximum cost is reduced, i.e.,

$$\begin{aligned} & \max \{f(\mathcal{R}_{m^*} \cap \{n\}, \omega_{m^*}), f(\mathcal{R}_{m^*} \setminus \{n\}, \omega_{m^-})\} \\ & < \max \left\{ \hat{f}(\mathcal{R}_{m^*}, \omega_{m^*}), \hat{f}(\mathcal{R}_{m^-}, \omega_{m^-}) \right\}, \end{aligned} \quad (10)$$

where $m^- = \mu_0(n)$ is the task to which agent n was assigned *before* applying the switch. Such a switch can be found by iterating through all agents within \mathcal{R}_{m^*} , and verifying whether the condition in (10) holds. Once a switch $\sigma_n^{m^*}$ is found, a new assignment is given by $\mu_1 = \sigma_n^{m^*}(\mu_0)$, after which a new target coalition can be found via (9). (II) If $f_{m^*} < \max_{m \neq m^*} \{\hat{f}_m\}$, it means that ω_{m^*} is no longer the target coalition based on its actual cost. Then, the estimated utility \hat{f}_{m^*} is updated accordingly and thus a new target coalition can be found via (9). The above procedure is repeated until the target coalition does not change anymore, of which the assignment and target coalition are denoted by μ_{K_1} and $(\omega_{m_1^*}, \mathcal{R}_{m_1^*})$, respectively.

Afterwards, the same process is repeated but focusing on the target coalition with *second* largest cost, i.e., by setting μ_{K_1} as the initial assignment and $k = 2$ instead in (9). Similarly, the procedure converges in this round after the target coalition remains unchanged. The same round is performed for $k = 3$ and so on until $k = M$, when the target coalition μ_{K_M} has the minimum utility. Note that if the target coalitions from the previous rounds, e.g., round k_1 , are changed during the current round $k_2 > k_1$, the whole process is re-started from $k = 1$.

Proposition 1. The final assignment μ_{K_M} is a Nash-stable assignment of \mathcal{F} under the actual cost function f .

Proof. (Sketch) First, the costs of all coalitions in μ_{K_M} are the actual cost derived by hybrid optimization. Second, the fact that no switch operations can be found for each agent fulfills the Nash-stable condition in Def. 3. □

B. Hybrid Optimization

As previously mentioned, the group of agents in \mathcal{R}_m as a coalition should follow a hybrid plan φ_m as defined in (2) to accomplish task ω_m . This section presents how such a hybrid can be found via the proposed hybrid optimization.

1) *Problem of Hybrid Optimization:* For the ease of notation, let $\mathbf{X} = x_{k_0^m} \cdots x_{k_T^m}$ be the sequence of system states at discrete time steps $t = 0, 1, \dots, T$ for a sufficient duration T ; $\Xi = \xi_{k_{t_1}^m}, \dots, \xi_{k_{t_N}^m}$ and $\mathbf{P} = \rho_{k_{t_1}^m}, \dots, \rho_{k_{t_N}^m}$ be the sequence of modes applied to the system for time periods $[t_0, t_1), [t_1, t_2), \dots, [t_{N-1}, t_N)$, where $t_n = nT_0, T_0 \in \mathbb{N}, \forall n = 0, \dots, \lfloor \frac{T}{T_0} \rfloor$. Note that $T_0 > 0$ is chosen as a lower bound on the duration of each mode to avoid too frequent switching of modes and parameters. Furthermore, let $\mathbf{X}_t, \Xi_t, \mathbf{P}_t$ denote $x_{k_t^m}, \xi_{k_t^m}, \rho_{k_t^m}$. Then, the hybrid optimization problem is stated as follows:

Problem 3. Given a task ω_m and the associated coalition \mathcal{R}_m , find the optimal sequences $(\mathbf{X}, \Xi, \mathbf{P})$ that solve the

hybrid optimization (HO) problem below:

$$\begin{aligned}
& \min_{\Xi, \mathbf{P}} \sum_{t=0}^T c_{\text{cont}}(\mathbf{X}_t, \mathbf{P}_t) \\
& \text{s.t. } \mathbf{X}_0 = x_0, \mathbf{X}_T \in \mathcal{X}_{G_m}; \\
& \xi_{k_t^m} = \Xi_{t_n}, \rho_{k_t^m} = \mathbf{P}_{t_n}, \forall t \in [t_n, t_{n+1}); \\
& \mathbf{X}_{t+1} = h_{\xi_{k_t^m}}(\mathbf{X}_t, \mathcal{R}_m, \mathbf{P}_t), \forall t \in [0, T];
\end{aligned} \tag{11}$$

where $c_{\text{cont}}(\cdot)$ is a general function including the control cost and smoothness; $h_{\xi_{k_t^m}}(\cdot)$ is the system dynamics under each mode from (1); and the constraints require that the mode and parameter are kept static within $[t_n, t_{n+1})$. ■

Note that different from the original combinatorial-hybrid optimization problem in (6), the goal of the hybrid optimization problem above is to find the optimal hybrid plan φ_m for a specific task ω_m and the corresponding coalition \mathcal{R}_m . A novel hybrid-search algorithm called Heuristic Gradient-Guided Hybrid Search (HGG-HS) is proposed to solve Problem 3. Instead of feeding the above problem directly into a general nonlinear optimizer, the proposed algorithm combines: (i) the A^* -based discrete search for the optimal sequence of modes, and (ii) the gradient-based optimization for the optimal sequence of parameters. More specifically, the hybrid search tree is defined as $\mathcal{T} \triangleq (V, E, \nu_0, V_G)$, where $V = \{\nu\}$ is a set of vertices for $\nu \in \mathcal{X}_{\text{safte}}$; $E \subset V \times V$ is a set of edges; $\nu_0 \in V$ is the initial vertex; and $V_G \subset V$ is a set of goal states determined by \mathcal{X}_{G_m} . Moreover, let $\text{cost}(\nu)$ be the cost of node ν and $\text{prev}(\nu)$ be the parent node of ν .

2) *Design of Heuristic Functions:* As stated in [28], a proper design of the heuristic function $h : \mathcal{X} \rightarrow \mathbb{R}^+$ is essential for the performance of the A^* search algorithm. Since it is impractical to find an exact heuristic function h^{opt} that estimates *perfectly* the cost from a given vertex $\nu \in V$ to the goal set V_G , this work proposes two approximations of the exact heuristics at different level of abstraction: (i) the global approximation h^G that serves as a lower bound on the actual cost, i.e., $h^{\text{opt}}(x) \geq h^G(x), \forall x \in \mathcal{X}$. For instance, Euclidean distance is a common choice as admissible heuristics; (ii) the local approximation h^L that is differentiable and has similar gradients to h^{opt} in a local neighborhood, i.e., $\|\nabla h_{x_0}^L(x) - \nabla h^{\text{opt}}(x)\| \leq E, \forall x \in \mathcal{U}_d(x_0) = \{x \in \mathcal{X} \mid \|x - x_0\| \leq d\}$ and $E > 0$. Furthermore, a balanced heuristic function h^B is defined recursively as follows:

$$h^B(\nu) = \lambda(h^B(\tilde{\nu}) + \Delta h^L(\tilde{\nu}, \nu)) + (1 - \lambda)h^G(\nu), \tag{12}$$

where $\tilde{\nu} = \text{prev}(\nu)$; $\lambda \in [0, 1]$ is a weighting factor; and $\Delta h(\tilde{\nu}, \nu)$ is the change of cost from $\tilde{\nu}$ to ν , which is estimated by the accumulated change along a path, i.e.,

$$\Delta h^L(\tilde{\nu}, \nu) = \sum_{\ell=1}^L (h_{x_\ell}^L(x_\ell) - h_{x_{\ell-1}}^L(x_{\ell-1})), \tag{13}$$

where $x_0 = \tilde{\nu}$, $x_L = \nu$, and $x_\ell \in \mathcal{U}_d(x_{\ell-1}), \forall \ell = 1, \dots, L$. Moreover, λ is a parameter that effects the greedy-ness of HGG-HS. Namely, when $\lambda = 0$ holds, h^B reduces to h^G , yielding a general heuristic search algorithm like A^* . On the

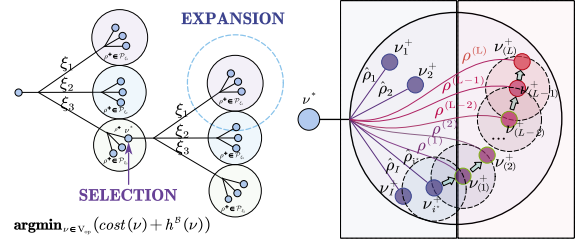


Fig. 4. Illustration of the hybrid search algorithm in Sec. IV-B.3: selection and expansion (Left); iterative parameter optimization (Right).

other hand, when $\lambda = 1$ holds, h^B only depends on the local approximation h^L , resulting in a local greedy search.

3) *Heuristic Gradient-Guided Hybrid Search:* Given the above definition of balanced heuristics, the hybrid search tree \mathcal{T} is explored via an iterative process of node selection and expansion. To begin with, similar to the A^* algorithm, a priority queue $V_{\text{op}} \subset V$ is used to store the vertices to be visited, while a set $V_{\text{c1}} \subset V$ is used to store the vertices that have been fully explored. Then, as illustrated in Fig. 4, the proposed hybrid search algorithm consists of the following stages: (I) **Selection.** The vertex with the lowest estimated cost in V_{op} is selected, i.e., $\nu^* = \arg\min_{\nu \in V_{\text{op}}} \{\text{cost}(\nu) + h^B(\nu)\}$, of which the associated state is x^* . (II) **Expansion.** This vertex ν^* is expanded in three steps: (i) first, a feasible mode $\xi \in \Xi$ is chosen given the state x^* ; (ii) then, a set of candidate parameters $\{\rho^*\} \subset \mathcal{P}_\xi$ is found for mode ξ and x^* via an iterative optimization in the parameter space as described in the sequel; (iii) lastly, given ξ and $\{\rho^*\}$ above, the set of resulting child vertices $\mathcal{C}_\xi(\nu^*) \triangleq \{\nu^+\}$ is given by:

$$\begin{aligned}
\mathbf{x}_{t+1} &= h_\xi(\mathbf{x}_t, \mathcal{R}_m, \rho^*), \forall t \in [0, T_0]; \\
x_0 &= x^*, \nu^+ = \mathbf{x}_{T_0};
\end{aligned} \tag{14}$$

which is encapsulated by $\nu^+ \triangleq \text{Expand}(x^*, \rho^*)$ for the ease of notation. Moreover, the properties of ν^+ is updated by $\text{cost}(\nu^+) = \text{cost}(\nu^*) + \sum_{t=0}^{T_0} c_{\text{cont}}(\mathbf{x}_t, \rho^*)$ and $\text{prev}(\nu^+) = \nu^*$. Each child node $\nu^+ \in \mathcal{C}_\xi(\nu^*)$ is added to the node set V and V_{op} , if $\nu \notin V_{\text{c1}}$ and $\text{cost}(\nu^+) \leq \text{cost}(\nu), \forall \nu \in V$ that satisfying $[(\nu^+ - \nu)/\delta] = \mathbf{0}$, where $[\cdot]$ is the rounding function for a radius $\delta > 0$. Afterwards, the edge (ν^*, ν^+) is added to the edge set E and labeled by the associated mode and parameter (ξ, ρ^*) . (III) **Termination.** If all the child vertices of ν^* have been explored, ν^* is removed from V_{op} and added to V_{c1} . More importantly, if $\nu^* \in V_G$ holds, the optimized sequences Ξ and \mathbf{P} as the solution to Problem 3 can be obtained by tracing back the parent vertices and retrieving its label (ξ, ρ) . Thus, the hybrid search algorithm returns the hybrid plan as described in (11), along with the actual cost for the assigned task.

4) *Iterative Optimization of Mode Parameters:* The optimization for parameter ρ^* in the stage of expansion above for node ν^* follows a two-stage process. In the first stage of *primitive expansion*, parameters are initially selected from a predefined set of primitive parameters $\{\hat{\rho}_1, \dots, \hat{\rho}_I\} \subset \mathcal{P}_\xi$. Then, a set of child vertices can be generated by $\nu_i^+ = \text{Expand}(x^*, \hat{\rho}_i), \forall \hat{\rho}_i \in \hat{\mathcal{P}}_\xi$. Within this set, the child vertex

with lowest estimated total cost is selected, i.e.,

$$\nu_{i^*}^+ = \mathbf{argmin}_{\nu \in \{\nu_i^+\}} \left\{ \text{cost}(\nu) + h^{\mathcal{B}}(\nu) + h^{\mathcal{L}}(\nu^*, \nu) \right\} \quad (15)$$

and the associated parameter is $\hat{\rho}_{i^*}$. In the second stage of *iterative optimization*, the end state $x_e^{(\ell)}$ and the associated parameter $\rho^{(\ell)}$ is optimized via nonlinear optimization for iterations $\ell = 1, \dots, L$. Initially, $x_e^{(0)} = \nu_{i^*}$ and $\rho^{(0)} = \hat{\rho}_{i^*}$. Then, the following procedure is applied to update $\rho^{(\ell)}$:

$$\rho^{(\ell+1)} = \mathbf{argmin}_{\rho \in \mathcal{P}_\xi} \left\{ \sum_{t=0}^{T_0} c_{\text{cont}}(\mathbf{x}_t) + h_{x_e^{(\ell)}}^{\mathcal{L}}(\mathbf{x}_{T_0}) \right\}; \quad (16)$$

$$\mathbf{s.t.} \quad \mathbf{x}_0 = \nu^*, \quad \mathbf{x}_{T_0} \in U_d(x_e^{(\ell)}) \text{ in (14),}$$

which can be solved by a general nonlinear optimization solver such as IPOPT [29], as all states are parameterized over ρ . Once $\rho^{(\ell+1)}$ is obtained, the associated end state is updated by $x_e^{(\ell+1)} = \text{Expand}(\nu^*, \rho^{(\ell+1)})$. This iterative process continues until iteration L such that $\|x_e^{(L)} - x_e^{(L-1)}\| < d$. Consequently, the set of pairs of parameters and end states is given by $\{(\rho^{(\ell)}, x_e^{(\ell)})\}$, of which the corresponding child vertices are $\{\nu_{(\ell)}^+\}$. Thus, the set of all child vertices $\mathcal{C}_\xi(\nu^*) = \{\nu_i^+, \forall i\} \cup \{\nu_{(\ell)}^+, \forall \ell\}$ is sent to the next step in the stage of expansion.

Theorem 1. Consider a path ν_0, \dots, ν_K of length K in \mathcal{T} obtained via the hybrid search algorithm. Then, $h_{k+1}^{\mathcal{B}} \leq (1 + \epsilon)h_{k+1}^{\text{opt}}$ holds, i.e., its cost is at most $(1 + \epsilon)$ times the minimum cost, if $\lambda_k \leq \frac{h_k^{\mathcal{G}}}{EJ/\epsilon + \Delta c_m + h_k^{\mathcal{G}}}$ in (12), $\forall k = 1, \dots, K$ and parameter $\epsilon \geq 0$.

Proof. For brevity, let $h_k^{\mathcal{B}}, h_k^{\mathcal{G}}, h_k^{\text{opt}}$ denote the various heuristics of vertex ν_k defined in (12), $c_k = \text{cost}(\nu_k)$ and $\Delta h_k^{\mathcal{L}} = \Delta h^{\mathcal{L}}(\nu_k, \nu_{k+1})$. To begin with, $h_0^{\mathcal{B}} = h_0^{\mathcal{G}} \leq (1 + \epsilon)h_0^{\text{opt}}$ holds due to the boundary condition in [28]. Assuming that $h_k^{\mathcal{B}} \leq (1 + \epsilon)h_k^{\text{opt}}$ is satisfied for any k . Then, $\Delta h_k^{\mathcal{L}}$ can be bounded as follows:

$$\begin{aligned} \Delta h_k^{\mathcal{L}} &= \sum_{\ell=0}^{L-1} (h_{x_e^{(\ell)}}^{\mathcal{L}}(x^{(\ell)}) - h_{x_e^{(\ell)}}^{\mathcal{L}}(x^{(\ell-1)})) \\ &\leq h_{k+1}^{\text{opt}} - h_k^{\text{opt}} + EJ, \end{aligned}$$

where $\|e(x)\| = \|\nabla h_{x_0}^{\mathcal{L}}(x) - \nabla h_{x_0}^{\text{opt}}(x)\| \leq E$; J is the maximum distance between a vertex and its parent vertex. Then, it can be derived that:

$$\begin{aligned} h_{k+1}^{\mathcal{B}} &= \lambda(h_k^{\mathcal{B}} + \Delta h_k^{\mathcal{L}}) + (1 - \lambda)(h_{k+1}^{\mathcal{G}}) \\ &\leq \lambda((1 + \epsilon)h_k^{\text{opt}} + \Delta h_k^{\mathcal{L}}) + (1 - \lambda)h_{k+1}^{\text{opt}} \quad (17) \\ &\leq (1 + \lambda\epsilon)h_{k+1}^{\text{opt}} + \lambda\epsilon\Delta c_m + \lambda EJ, \end{aligned}$$

where $h_k^{\text{opt}} < h_{k+1}^{\text{opt}} + \Delta c$ and $\Delta c = c_{k+1} - c_k < c_m$. If $\lambda \leq \frac{h_{k+1}^{\mathcal{G}}}{EJd/\epsilon + \Delta c_m + h_{k+1}^{\mathcal{G}}}$ holds, combining with (17) implies $h_{k+1}^{\mathcal{B}} \leq (1 + \epsilon)h_{k+1}^{\text{opt}}$. Thus, via induction over k , $h_K^{\mathcal{B}} \leq (1 + \epsilon)h_K^{\text{opt}}$ holds, which ensures a bounded sub-optimality. \square

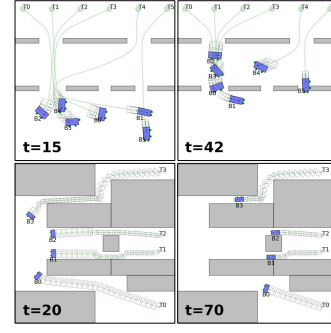


Fig. 5. Snapshots of collaborative transportation within two scenarios: 16 agents (blue circles) for 6 boxes (Top); 10 agents for 4 boxes (Bottom).

C. Overall Framework

As described in Sec. IV-A.2, the two layers are executed in an interleaved and concurrent way. More specifically, the layer of coalition formation searches for the appropriate switch operations to reduce the overall cost in (8) of an assignment μ . During this process, whenever the actual cost f_m of a coalition \mathcal{R}_m for task ω_m is required, the layer of hybrid optimization searches for the optimal sequence of modes and parameters (Ξ_m, \mathbf{P}_m) for the coalition \mathcal{R}_m to accomplish ω_m , while minimizing the actual cost. This process repeats itself until no such switch operations can be found and the costs of all coalitions have been verified by the hybrid optimization. The resulting assignment is given by μ^* and the optimal plan is $(\Xi_m^*, \mathbf{P}_m^*)$ for each task $\omega_m \in \Omega$. Thus, the final hybrid plan in (2) for ω_m is given by:

$$\varphi_m^* = (\xi_{k_1}^*, \mathcal{R}_m, \rho_{k_1}^*) \cdots (\xi_{k_N}^*, \mathcal{R}_m, \rho_{k_N}^*), \quad (18)$$

where $\Xi_m^* = \xi_{k_1}^* \cdots \xi_{k_N}^*$ and $\mathbf{P}_m^* = \rho_{k_1}^* \cdots \rho_{k_N}^*$, and the total length varies across different tasks. Given these hybrid plans, each agent $n \in \mathcal{N}$ can start executing the assigned task $\mu^*(n)$, by following the optimal sequence of modes with the chosen parameters. Due to unforeseen disturbances and uncertainties, the system state may evolve differently from the planned trajectory, in which case the task assignment and hybrid plans should be updated by resolving Problem 1 given the current system state.

V. NUMERICAL EXPERIMENTS

To further validate the proposed method, extensive numerical simulations are presented in this section. The proposed method is implemented in Python3 and tested on a laptop with an Intel Core i7-1280P CPU.

A. Collaborative Transportation

1) *Experiment Setup:* As introduced in Sec. III-A and shown in Fig. 5, the workspace of size $10m \times 10m$ is cluttered with rectangular obstacles. There are 16 agents and 6 boxes randomly distributed within the workspace. Each box has a size of $1m \times 0.5m$, and the circular agents have a radius $r = 0.1m$. For simplicity, each robot has a first-order dynamics and can provide bounded pushing force at specific points of the box, thus changing the state of boxes with second-order translational invariant dynamics. Note that the cluttered workspace introduces severe geometric constraints,

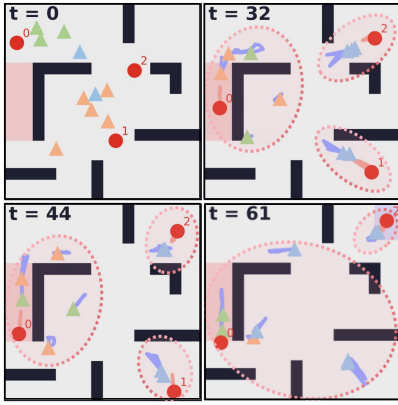


Fig. 6. Snapshots of simulated dynamic capture. Pursuers (triangles) are encircled by their coalitions and the assigned evader (red circles).

yielding a significantly more difficult transportation task than the obstacle-free environments [19], [20]. Initially, the task cost $f(\cdot)$ in (7) is estimated by the sum of Euclidean distances from agents to the targeted box, and the distance to its goal position. The heuristic function $h^G(x)$ is designed as the minimum distance from state x to \mathcal{X}_{G_m} , estimated by the A^* search, and $h^L(x)$ is designed as the kinematic cost under the local geometry constraints from current state x to next intermediate region $\hat{\mathcal{X}}$ on the shortest path.

2) *Results*: Evolution of the system state is shown in Fig. 5. Initially, the coalition formation for 6 tasks and 16 agents takes 9s, during which 16 hybrid search problems are solved in the hybrid optimization layer. It can be seen that different modes have a significant influence on overall cost. e.g., box 5 reaches its goal location faster by choosing a short-side pushing mode with 2 agents to pass through a narrow passage; 3 agents are assigned to box 4 such that it can be pushed through 2 passages that are far away; box 5 is pushed to its target by 4 agents via almost a straight line. To further validate the applicability, another complex scenario is considered and shown in Fig. 5, where numerous sharp turns are required for the boxes to arrive at the destinations. Consequently, more frequent mode switchings can be found in the final solution, e.g., the coalition of 4 agents associated with box 3 switches the mode from the “long side” to the “short side”, such that the box could pass through the first passage at $t = 45s$. However, since pushing from a narrow side introduces higher kinematic uncertainty and thus larger cost, the same coalition switches to the “diagonally pushing” mode after passing through the second passage at $t = 92s$. Furthermore, for both boxes 1 and 2, two agents switch from “long-side” to “short-side” for the middle passage at $t = 70$.

B. Dynamic Capture

1) *Experiment Setup*: As introduced in Sec. III-B and shown in Fig. 6, the workspace contains randomly placed obstacles of various shapes like corridors and corners, yielding a much more difficult capture task than the obstacle-free environments [3], [24]. There are 10 pursuers and 3 evaders randomly distributed in a workspace of size $2.5m \times 2.5m$. For simplicity, all agents satisfy the single-integrator dynamics, with the same maximum velocity of $4m/s$. The system state

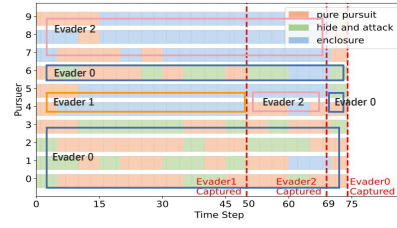


Fig. 7. Evolution of task and modes for dynamic capture during one run.

is available at all time for the pursuers. The capture radius of pursuers is set to $0.15m$. As described in Sec. III-B, the pursuers follow three parameterized modes to capture the evaders in a collaborative way. The task cost $f(\cdot)$ in (7) is estimated by the weighted average distance from the pursuers in a coalition to the assigned evader. Heuristics $h^G(\cdot)$ is designed as the minimum distance to the evader, and $h^L(\cdot)$ is designed according to specific local environments, e.g., the area of the corner envelop for enclosure mode. Lastly, the parameter associated with mode of “pure pursuit” is determined solely by the position of the targeted evader; the parameter for the mode of “hide and attack” is sampled from a set of potential locations given the workspace layout and the targeted evader; the parameter for the mode of “enclosure” is determined by maximizing the region of advantage [25].

2) *Results*: The first layer of task allocation process is executed every 15 time steps, while the layer of hybrid optimization is updated every 5 time steps to adapt to the fast movement of evaders. Evolution of the system under one solution is visualized in Fig. 6. Initially, the position of pursuers and evaders are initialized randomly. As shown in Fig. 7, pursuers 0, 1, 2, 3 and 6 are assigned to capture evader 0 initially, while pursers 4, 5 captured evader 1, and pursers 7, 8, 9 for evader 2. At $t = 50$, evader 1 is captured under the mode “enclosure” by setting the parameters as even dividers on the boundary of advantage region. Afterwards, pursuers 4, 5 join the coalition for evader 2 with the mode “pure pursuit”. Then, evader 2 is captured at $t = 69$ under the mode “enclosure”, after which pursuers 4, 5 join the coalition for evader 0 with the mode “hide and attack”. It can be seen that the selected parameters for this mode are mainly located around the four corners of obstacles in the middle. All evaders are captured at $t = 75$, during which there are in total 3 switches of tasks and 24 switches of modes.

C. Comparisons

Effectiveness of the proposed method for the case of object transportation is compared against two baselines: (i) the Greedy Assignment (GA), where each task is assigned to one closest free agent sequentially until each agent has an assigned task; (ii) Fixed Mode (FM) where all coalitions follow only one mode, and the layer of coalition formation remains the same. The main metrics to compare are the sum of the cost of the hybrid plans for all coalitions and the time when all tasks are completed.

As summarized in Table I, for the task of collaborative transportation, our algorithm surpasses both baselines in every metric, e.g., the GA and FM methods have an

Case	Method	Average Time (sec)	Mean Cost
Collaborative Transportation	GA	127.8	20.6
	FM	132.7	26.1
	Ours	108.5	19.0
Dynamic Capture	GA	186	10.7
	FM	108	6.0
	Ours	74	5.7

TABLE I
COMPARISON WITH TWO BASELINES.

average completion time of 127.8s and 132.7s, which is much higher than 108.5s of our method. The FM method takes considerably more time than ours in this case, as the switching of different modes is essential for the task completion. Secondly, for the task of dynamic capture, it takes around 74 time steps for our method to capture all evaders, with the minimum and maximum capture time being 70 and 80 steps. In comparison, the FM method has a much longer capture time of 108 steps, while the GA method takes even longer with 186 steps in average. It is interesting to notice that under the GA method subgroups of pursuers often target the same evader that are close and ignore other evaders, causing an unbalanced assignment.

VI. CONCLUSION

This work proposes a combinatorial-hybrid optimization (CHO) framework for multi-agent systems under collaborative tasks. The proposed approach solves simultaneously the coalition formation and the hybrid optimization of collaborative behaviors, with a provable quality guarantee. Future work involves the consideration of uncertain environments.

REFERENCES

- [1] T. Bock, "Construction robotics," *Autonomous Robots*, vol. 22, no. 3, pp. 201–209, 2007.
- [2] M. Krizmancic, B. Arbanas, T. Petrovic, F. Petric, and S. Bogdan, "Cooperative aerial-ground multi-robot system for automated construction tasks," *IEEE Robotics and Automation Letters*, vol. 5, no. 2, pp. 798–805, 2020.
- [3] A. Pierson, Z. Wang, and M. Schwager, "Intercepting rogue robots: An algorithm for capturing multiple evaders with multiple pursuers," *IEEE Robotics and Automation Letters*, vol. 2, no. 2, pp. 530–537, 2016.
- [4] A. Khan, B. Rinner, and A. Cavallaro, "Cooperative robots to observe moving targets," *IEEE transactions on cybernetics*, vol. 48, no. 1, pp. 187–198, 2016.
- [5] A. Torreño, E. Onaindia, A. Komenda, and M. Štolba, "Cooperative multi-agent planning: A survey," *ACM Computing Surveys (CSUR)*, vol. 50, no. 6, pp. 1–32, 2017.
- [6] M. Gini, "Multi-robot allocation of tasks with temporal and ordering constraints," in *AAAI Conference on Artificial Intelligence*, 2017.
- [7] R. Massin, C. J. Le Martret, and P. Ciblat, "A coalition formation game for distributed node clustering in mobile ad hoc networks," *IEEE Transactions on Wireless Communications*, vol. 16, no. 6, pp. 3940–3952, 2017.
- [8] I. E. Weintraub, M. Pachter, and E. Garcia, "An introduction to pursuit-evasion differential games," in *IEEE American Control Conference (ACC)*, 2020, pp. 1049–1066.
- [9] J. Tordesillas and J. P. How, "Mader: Trajectory planner in multiagent and dynamic environments," *IEEE Transactions on Robotics*, vol. 38, no. 1, pp. 463–476, 2021.
- [10] V. R. Makkapati and P. Tsiotras, "Optimal evading strategies and task allocation in multi-player pursuit-evasion problems," *Dynamic Games and Applications*, vol. 9, pp. 1168–1187, 2019.

- [11] V. N. Hartmann, O. S. Oguz, D. Driess, M. Toussaint, and A. Menges, "Robust task and motion planning for long-horizon architectural construction planning," in *IEEE/RSJ International Conference on Intelligent Robots and Systems (IROS)*, 2020, pp. 6886–6893.
- [12] A. Khamis, A. Hussein, and A. Elmogy, "Multi-robot task allocation: A review of the state-of-the-art," *Cooperative Robots and Sensor Networks 2015*, pp. 31–51, 2015.
- [13] R. Fukasawa, H. Longo, J. Lysgaard, M. P. De Aragão, M. Reis, E. Uchoa, and R. F. Werneck, "Robust branch-and-cut-and-price for the capacitated vehicle routing problem," *Mathematical programming*, vol. 106, no. 3, pp. 491–511, 2006.
- [14] E. Nunes and M. Gini, "Multi-robot auctions for allocation of tasks with temporal constraints," in *AAAI Conference on Artificial Intelligence*, vol. 29, no. 1, 2015.
- [15] R. Jonker and T. Volgenant, "Improving the hungarian assignment algorithm," *Operations Research Letters*, vol. 5, no. 4, pp. 171–175, 1986.
- [16] K. R. Apt and A. Witzel, "A generic approach to coalition formation," *International game theory review*, vol. 11, no. 03, pp. 347–367, 2009.
- [17] E. Soria, F. Schiano, and D. Floreano, "Distributed predictive drone swarms in cluttered environments," *IEEE Robotics and Automation Letters*, vol. 7, no. 1, pp. 73–80, 2021.
- [18] X. Sun and C. G. Cassandras, "Optimal dynamic formation control of multi-agent systems in constrained environments," *Automatica*, vol. 73, pp. 169–179, 2016.
- [19] E. Tuci, M. H. Alkilabi, and O. Akanyeti, "Cooperative object transport in multi-robot systems: A review of the state-of-the-art," *Frontiers in Robotics and AI*, vol. 5, p. 59, 2018.
- [20] K. I. Alevizos, C. P. Bechlioulis, and K. J. Kyriakopoulos, "Bounded energy collisions in human–robot cooperative transportation," *IEEE/ASME Transactions on Mechatronics*, vol. 27, no. 6, pp. 4541–4549, 2022.
- [21] M. Guo, J. Tumova, and D. V. Dimarogonas, "Communication-free multi-agent control under local temporal tasks and relative-distance constraints," *IEEE Transactions on Automatic Control*, vol. 61, no. 12, pp. 3948–3962, 2016.
- [22] M. Guo and M. M. Zavlanos, "Multirobot data gathering under buffer constraints and intermittent communication," *IEEE transactions on robotics*, vol. 34, no. 4, pp. 1082–1097, 2018.
- [23] M. Dogar, A. Spielberg, S. Baker, and D. Rus, "Multi-robot grasp planning for sequential assembly operations," *Autonomous Robots*, vol. 43, pp. 649–664, 2019.
- [24] M. Chen, Z. Zhou, and C. J. Tomlin, "Multiplayer reach-avoid games via pairwise outcomes," *IEEE Transactions on Automatic Control*, vol. 62, no. 3, pp. 1451–1457, 2016.
- [25] A. Von Moll, D. W. Casbeer, E. Garcia, and D. Milutinović, "Pursuit-evasion of an evader by multiple pursuers," in *International Conference on Unmanned Aircraft Systems (ICUAS)*, 2018, pp. 133–142.
- [26] T. Rahwan, T. P. Michalak, M. Wooldridge, and N. R. Jennings, "Coalition structure generation: A survey," *Artificial Intelligence*, vol. 229, pp. 139–174, 2015.
- [27] Q. Li, M. Li, B. Q. Vo, and R. Kowalczyk, "An anytime algorithm for large-scale heterogeneous task allocation," in *International Conference on Engineering of Complex Computer Systems (ICECCS)*, 2020, pp. 206–215.
- [28] S. Cui, X. Jin, S. Wang, Y. He, and Q. Huang, "Heuristic domain adaptation," *Advances in Neural Information Processing Systems*, vol. 33, pp. 7571–7583, 2020.
- [29] A. Wächter, "Short tutorial: Getting started with ipopt in 90 minutes," in *Dagstuhl Seminar Proceedings*. Schloss Dagstuhl-Leibniz-Zentrum fuer Informatik, 2009.